NGU Report 2007.001

Refinement of phosphorus determination in quartz by LA-ICP-MS through defining new reference material values

NGU
Norges geologiske undersøkelse
Geological Survey of Norway

Geological Survey of Norway
NO-7491 Trondheim, Norway
Tel.: 47 73 90 40 00
Telefax 47 73 92 16 20

REPORT

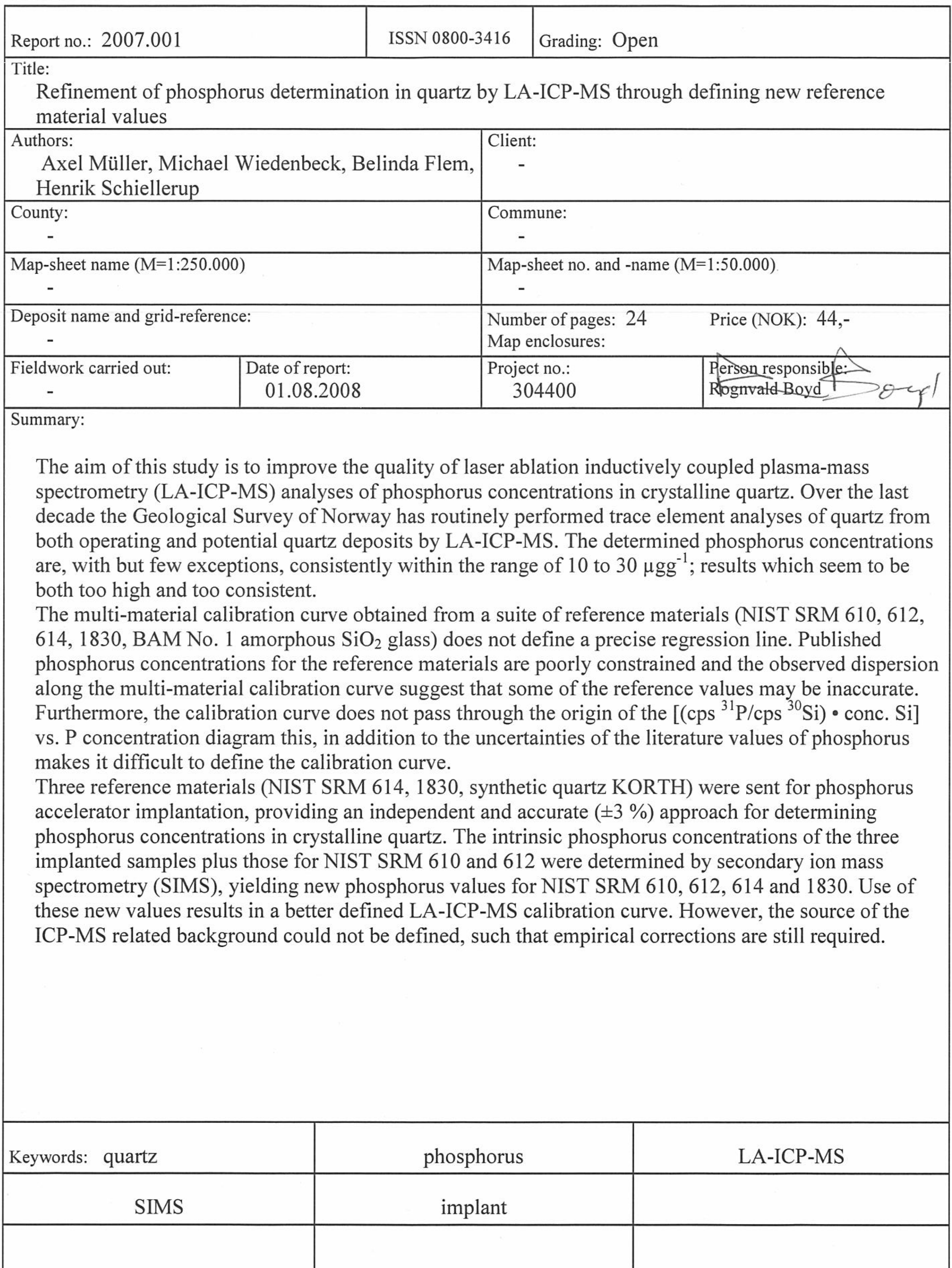

Report no.: 2007.001	ISSN 0800-3416	Grading: Open

Title:
Refinement of phosphorus determination in quartz by LA-ICP-MS through defining new reference material values

Authors:	Client:
Axel Müller, Michael Wiedenbeck, Belinda Flem, Henrik Schiellerup	-
County: -	Commune: -
Map-sheet name (M=1:250.000) -	Map-sheet no. and -name (M=1:50.000) -
Deposit name and grid-reference: -	Number of pages: 24 Price (NOK): 44,- Map enclosures:

Fieldwork carried out:	Date of report:	Project no.:	Person responsible:
-	01.08.2008	304400	Rognvald Boyd

Summary:

The aim of this study is to improve the quality of laser ablation inductively coupled plasma-mass spectrometry (LA-ICP-MS) analyses of phosphorus concentrations in crystalline quartz. Over the last decade the Geological Survey of Norway has routinely performed trace element analyses of quartz from both operating and potential quartz deposits by LA-ICP-MS. The determined phosphorus concentrations are, with but few exceptions, consistently within the range of 10 to 30 $\mu g g^{-1}$; results which seem to be both too high and too consistent.
The multi-material calibration curve obtained from a suite of reference materials (NIST SRM 610, 612, 614, 1830, BAM No. 1 amorphous SiO_2 glass) does not define a precise regression line. Published phosphorus concentrations for the reference materials are poorly constrained and the observed dispersion along the multi-material calibration curve suggest that some of the reference values may be inaccurate. Furthermore, the calibration curve does not pass through the origin of the [(cps ^{31}P/cps ^{30}Si) • conc. Si] vs. P concentration diagram this, in addition to the uncertainties of the literature values of phosphorus makes it difficult to define the calibration curve.
Three reference materials (NIST SRM 614, 1830, synthetic quartz KORTH) were sent for phosphorus accelerator implantation, providing an independent and accurate (±3 %) approach for determining phosphorus concentrations in crystalline quartz. The intrinsic phosphorus concentrations of the three implanted samples plus those for NIST SRM 610 and 612 were determined by secondary ion mass spectrometry (SIMS), yielding new phosphorus values for NIST SRM 610, 612, 614 and 1830. Use of these new values results in a better defined LA-ICP-MS calibration curve. However, the source of the ICP-MS related background could not be defined, such that empirical corrections are still required.

Keywords: quartz	phosphorus	LA-ICP-MS
SIMS	implant	

CONTENTS

1. Introduction 5
2. Experimental methods 7
   2.1 Laser ablation inductively coupled plasma-mass spectrometry 7
   2.2 Secondary ion mass spectrometry (SIMS) 8
   2.3 Solution ICP-MS 10
      2.3.1 HF-$HClO_4$ decomposition procedure 10
      2.3.2 Method of standard addition 10
   2.4 WDS analysis of NIST SRM 610 10
3. Re-evaluation of phosphorus values of RMs 11
   3.1 Published phosphorus values of RM 11
   3.2 Phosphorus analyses of NIST SRM glasses by solution ICP-MS and WDS 13
   3.3 Phosphorus analyses of NIST SRM glasses by SIMS 14
   3.4 Proposed new phosphorus values for NIST SRM 610, 612, 614, and 1830 16
4. Discussion of the ICP-MS related background at mass ^{31}P 17
   4.1 Spectroscopic interference of ^{31}P with silicon hybrids and other compounds created during ionization 17
   4.2 Spectroscopic interference of the internal standard ^{30}Si 17
   4.3 Phosphorus fractionation during ablation, transport and ionization 17
   4.4 Other possible causes of the ICP-MS related background 19
5. Conclusions and outlook 21
6. Acknowledgements 21
7. References 22

FIGURES

Figure 1. *Depth vs. concentration distribution of implanted 31P in crystalline SiO2 applying 100 keV and 5x1014 31P ions/cm2 based on ion-atom simulation calculation (www.srim.org). Logarithmic graph.* 9

Figure 2. *Example of multi-RM calibration curve (weighted linear regression). The dashed line is the regression line calculated from [(cps ^{31}P/cps ^{30}Si) • conc. Si] values and recommended P values of the RMs NIST SRM 610, 612, 614, 1830, and BAM No.1 ("*"-values in Table 1). The P value for the BAM No.1 is set to 1 µgg^{-1} (Table 1) to have a RM with very low P. Each RM was analyzed two times. The solid line represents the regression forced through the zero intercept of the diagram by ignoring the intensities of NIST SRM 614, 1830, and BAM No.1. This procedure has been applied at the NGU for calculation of P concentrations in quartz in past years. Uncertainty bars are the standard deviations of the compiled RM P concentrations and calculated from the uncertainties of the ^{30}Si and ^{31}P signal intensities.* 13

Figure 3. *An example of a profile analysis for the ^{31}P-implanted NIST SRM 1830. By assuming a constant sputtering rate and knowing the total duration and final depth of the analysis, the peak implant depth can be estimated at ~140 nm.* 15

Figure 4. *Multi-standard calibration curve (black dashed line) applying the newly compiled P values of the RMs NIST SRM 610, 612, 614, and 1830. The dataset is the same as in Figure 2 shown as gray diamonds and lines in the background. The black solid line represents the weighted linear regression with corrected intercept b.* 16

Figure 5. *Resolution of mass peaks around ^{31}P during ablation of NIST SRM 610 at medium mass resolution (m/Δm = 3500).* 17

TABLES

Table 1. *Published and newly compiled P concentrations of 7 reference materials. Concentrations marked with * have been previously used for multi-RM calibration at the NGU (Figure 2). Newly compiled P values are on black background. Analyses and compiled values on grey background are not considered in the calculation of the newly compiled P values. n – number of analyses, unc. – uncertainty, SD - standard deviation, SE - standard error.* 6

Table 2. *Operating parameters of the ICP-MS and key method parameters.* 8

Table 3. *ICP-MS instrumental key parameters.* 10

Table 4. *Relative sensitivity factors (RSF) of 31P-implanted reference materials and the calculated P content (Pcalc) of these samples. SD – standard deviation of the P concentration.* 15

Table 5. *Ratios and absolute concentrations of P in NIST SRM 610, 612, and 614 determined by SIMS and compared with recommended concentration values by Pearce et al. (1997) and Gao et al. (2002).* 15

Table 6. *Ar-He background, ^{31}P intensity with subtracted Ar-He background, the [(cps ^{31}P/cps ^{30}Si) • conc. Si] value (^{30}Si-normalized ^{31}P signal intensity) of RMs, and parameters of the calibration curve (weighted regression: slope a, intercept b, correlation coefficient R2) obtained during the last three years at NGU b corr – corrected intercept by adapting to the P concentration of the Qz-Tu quartz and BAM No. 1 to 1 $\mu g g^{-1}$, LOD – limit of detection (3 sigma), LOD sample – reference sample used for LOD determination, SiO_2 bl. – SiO_2 blank sample, sequ. – analysis sequence, n – number of scans, * - SiO_2 blank with <1 $\mu g g^{-1}$ P were analyzed in place of Qz-Tu.* 20

1. Introduction

The driving factor behind this study is the increasing industrial demand for quartz raw material with very low P concentrations. Phosphorus (along with Al, Fe, B, Ti, and V) is a critical impurity in high purity quartz (HPQ) used as a starting material for the manufacture of semiconductor-grade silicon, photovoltaic materials and various frequency-control devices. The total content of such electrically active impurities in, e.g., solar-grade silicon products must lie in the range 0.1-10 $\mu g g^{-1}$ (Dietl et al. 1981). In trace amounts, P and B are used as dopants for semiconductors in order to provide free charge carriers. Together these elements can define the electro-physical properties of silica-based materials. Therefore, very low P and B concentrations in the quartz raw material are crucial for the quality of the final product.

There are few published data about P concentrations in crystalline quartz. Schrön et al. (1982) report P concentrations between 20 and 267 $\mu g g^{-1}$ (simple mean 58 $\mu g g^{-1}$, n = 31) in hydrothermal quartz from the Erzgebirge, Germany. Phosphorous in these samples was determined photometrically with the molybdenum-blue method according to Dick and Tabatabai (1977). A study by Dash et al. (2004) reported 0.8 to 8 $\mu g g^{-1}$ P in high purity quartz using ion chromatography.

Over the last decade the Geological Survey of Norway (NGU) has routinely performed in situ trace element analyses of quartz from operating and potential quartz deposits by LA-ICP-MS (Flem et al. 2002). Phosphorous concentrations determined by LA-ICP-MS at the NGU are very consistently within the range of 10 to 30 $\mu g g^{-1}$ (e.g., Ihlen et al. 2001, 2002, 2003, 2005, Wanvik 2003, 2004, Larsen et al. 2004) with only a few exceptions. Such concentrations seem both too high and too consistent, possibly suggestive of a method-related background.

The aim of this study is to improve both the accuracy and limit of quantification of in situ P determination in crystalline quartz by LA-ICP-MS. The P concentrations in NIST SRM 610, 612, 614, and 1830 glasses were determined by SIMS, solution ICP-MS and WDS. Additionally, ^{31}P-implanted NIST SRM 614 and 1830 glasses and synthetic quartz (KORTH) were used to calibrate SIMS analyses independently from published reference P values of these reference materials (RMs). These results have allowed us to significantly refine the calibration curve for determination of low P concentrations in natural quartz. Finally, the possible sources of the ICP-MS-related background are also discussed

Table 1. *Published and newly compiled P concentrations of 7 reference materials. Concentrations marked with * have been previously used for multi-RM calibration at the NGU (Figure 2). Newly compiled P values are on black background. Analyses and compiled values on grey background are not considered in the calculation of the newly compiled P values. n – number of analyses, unc. – uncertainty, SD - standard deviation, SE - standard error.*

standard	Author	method	external RM	n	value (µgg^{-1})	unc. (µgg^{-1})	unc. type
NIST SRM 610	Pearce *et al.* (1997)	solution ICP-MS	synthetic solution	1	304.9	54	SD
	Pearce *et al.* (1997)	mean	-	2	342.5*	53	SD
	Gao *et al.* (2002)	LA-ICP-MS	NIST SRM 610	134	343	13	SD
	Hollocher and Ruiz (1995)	EPMA	apatite	10	524	87	SD
	Pearce *et al.* (1997)	ICP-AES	synthetic solution	1	380	9	SD
	Rocholl *et al.* (1997)	LIMS	?	1	417	29	SD
	this study	WDS	apatite	3	427	50	SD
	this study	solution ICP-MS	standard addition	1	421	43	SD
	this study	SIMS	P-implanted NIST SRM 614	10	398	35	SD
	this study	**compiled**		**16**	**409**	**20**	**SD**
NIST SRM 612	Pearce *et al.* (1997)	solution ICP-MS	standard addition	1	71.2	21.7	SD
	Pearce *et al.* (1997)	mean	-	2	55.2*	22.7	SD
	Sylvester (2001)	compiled	-	?	45	?	?
	Spandler *et al.* (2003)	compiled	-	?	55	?	?
	Jochum *et al.* (2005)	compiled	-	?	51	6	SD
	Pearce *et al.* (1997)	ICP-AES	synthetic solution	1	39.1	0.6	SD
	Gao *et al.* (2002)	LA-ICP-MS	NIST SRM 610	1	56	7	SD
	Yuan *et al.* (2004)	LA-ICP-MS	NIST SRM 610	4	46	3	SD
	this study	solution ICP-MS	standard addition	2	50	6	SD
	this study	SIMS	P-implanted NIST SRM 614	10	38.3	2	SD
	this study	**compiled**		**18**	**45.9**	**8**	**SD**
NIST SRM 614	Jochum *et al.* (2005)	compiled	-	7	13	5	SD
	Gao *et al.* (2002)	LA-ICP-MS	NIST SRM 610	1	9.3*	0.1	SD
	Horn *et al.* (1997)	SIMS	NIST SRM 612	2	11.8	0.1	SE
	Yuan *et al.* (2004)	LA-ICP-MS	NIST SRM 610	4	18	2	SD
	this study	solution ICP-MS	standard addition	1	8	2	SD
	this study	SIMS	P-implanted NIST SRM 614	10	8.5	0.8	SD
	this study	**compiled**		**18**	**11.1**	**4**	**SD**
NIST SRM 1830	Flem and Bédard (2002)	LA-ICP-MS	NIST SRM 612, 614	8	18.4*	0.8	SE
	this study	**SIMS**	P-implanted NIST SRM 1830	**10**	**16.6**	**1.5**	**SD**
BAM No. 1 SiO_2 glass	Federal Institute for materials and testing (BAM)	photometry	?	4	<1*		
synth. quartz Qz-Tu	Müller, unpublished data	LA-ICP-MS	NIST SRM 610, 612, 614, 1830	100	<1*		
synth. quartz KORTH	Wiedenbeck, unpublished data	SIMS	NIST SRM 610	1	0.13	0.02	SD
	this study	**SIMS**	**P-implanted syn. quartz KORTH**	**2**	**0.41**	**0.12**	**SD**

2. Experimental methods

2.1 Laser ablation inductively coupled plasma-mass spectrometry

The ICP-MS used in this study is a double focusing sector field instrument (ELEMENT-1, Finnigan MAT, Bremen, Germany), which has been described in detail by Gießmann and Greb (1994) and Feldmann et al. (1994). The configuration used in this work includes the CD-2 Guard Electrode. A Finnigan MAT, UV laser probe operating at 266 nm with a Gaussian beam profile, as described by Schroeder et al. (1998), was used for ablation. A repetition rate of 20 Hz, and pulse energy of 0.7-0.8 mJ were applied. The laser was not equipped with an aperture, such that the laser beam needed to be optically focused to give a spot size of approximately 30 µm. Sample and RMs were ablated using raster technique and He carrier gas was used so as to enhance transport efficiency of ablated material (Günther and Heinrich 1999). The He carrier gas was mixed with Ar as a make-up gas before entering the ICP-MS in order to maintain optimum, stable excitation conditions. Key operating parameters of the laser probe and the ICP-MS are summarized in Table 2. This laser set-up can encounter difficulties in controlling ablation diameter and ablation depth. The ablation parameters had therefore to be carefully selected. We note that a shorter wavelength laser (e.g., an eximer or Nd:YAG laser operating at 193 nm) operated in conjunction with an aperture for the precise control of spot size and with a flat beam profile yielding flat craters would be expected to enhance data quality.

The presence of isobaric interferences with the mass of 31P required the use of medium mass resolution (m/Δm ~3500). The isotope ^{30}Si was used as an internal standard. In addition, the argide 40Ar2+ was measured between each sample in order to correct for time-dependant instrumental mass drift.

External calibration was done using three silicate glass reference materials produced by the National Institute of Standards and Technology, USA (NIST SRM 610, 612, and 614). In addition, NIST SRM 1830 soda-lime float glass (0.1 wt.% Al2O3) and the certified reference material BAM No.1 amorphous SiO2 glass from the Federal Institute for Material Research and Testing, Germany, were used. Certified, recommended and proposed values for the reference materials are taken from the certificates of analysis when available, or otherwise from Pearce et al. (1997), Horn et al. (1997), Gao et al. (2002) and Flem and Bédard (2002). Each measurement consisted of 15 scans, each 0.15 s of 31P and 20 other mass stations which are analyzed routinely together with 31P. In order to account for memory effects an Ar-He-blank was run before every measurement and this signal was subtracted from the instrumental 31P signal intensity prior to normalization against the internal standard. A weighted linear regression model, including two measurements of the different RMs, was used to define a calibration curve.

Ten sequential measurements on the "Qz-Tu" synthetic pure quartz monocrystal or on a "SiO2 blank" crystal were used to estimate the limit of detection (LOD) of phosphorus. LOD is based on 3 times standard deviation (3σ) of the 10 measurements. LOD for P vary between 1 and 9.4 µgg-1 depending on the specific conditions on the analysis day. The corresponding limits of quantification are 3.3 to 31.3 µgg^{-1} (10σ; Potts 1997).

Table 2*. Operating parameters of the ICP-MS and key method parameters.*

laser parameters	
Wavelength	266 nm
pulse width	3 ns (Q-switched)
pulse energy	0.7-0.8 mJ
ablated raster area	~140 x 200 µm
spot size	~30 µm
laser repetition rate	20 Hz
sample helium flow rate	~0.5 – 0.6 l/min
ICP-MS parameters	
plasma power	974
auxiliary gas flow	~1.2 l/min
sample gas flow	~0.9 1 l/min
Cone	high performance Ni
CD-2 guard electrode	Yes
data collection	
scan type	E-scan
no. of scans	15

2.2 Secondary ion mass spectrometry (SIMS)

SIMS is an alternative method to LA-ICP-MS for high precision in situ analyses of trace elements in quartz (e.g., Müller et al. 2003). Like LA-ICP-MS, SIMS is a comparative technique for which well-characterized RMs are essential. The main limitation of SIMS is that secondary ion yields are extremely matrix-dependent. Therefore, the determination of absolute P concentrations in quartz requires the availability of quartz RMs of confirmed homogeneity and known P composition. Unfortunately no quartz RM with a well-defined P concentration is currently available. Hence, the NIST SRM glasses seem to be the only alternative, which is not a fully satisfactory calibration approach.

In order to solve this problem we sent the three RMs - NIST SRM 614, NIST SRM 1830 and a high purity synthetic α-quartz - for accelerator-based ^{31}P implantation. The implantation of P of a known dose into quartz and glasses provides an independent means for accurately calibrating (circa ±20 µgg^{-1}) determinations of the P content in SiO_2. Sample mounts containing a synthetic quartz crystal (Korth Kristalle GmbH 2007) along with NIST SRMs 614 and 1830 were polished to a surface roughness <20 nm using 0.25 µm polycrystalline diamond powder followed by a 30-nm neutral alumina suspension. The samples were cleaned in high-purity ethanol, dried in air at ~70ºC and then sent for commercial 31P ion implantation (Panalytic GmbH Dresden 2007). ^{31}P ions were implanted with 100 keV (uncertainty in energy <1%) and a ^{31}P dose of 5x1014 ions/cm^2 (uncertainty in dose <3%). Based on ion-atom interaction simulations (www.srim.org), the maximum implant depth of ^{31}P into crystalline SiO_2 is circa 280 nm (Figure 1); it should be noted that this value may be slightly different for the NIST SRM 614 and 1830.

We used the Cameca ims 6f SIMS in Potsdam in order to assess P concentrations in crystalline quartz, in existing RMs and in 31P-implanted samples. Prior to SIMS measurements the samples were ultrasonically cleaned for five minutes in ethanol, dried in an oven and subsequently coated with a ca. 35 nm thick conductive high-purity Au film. The sample material was sputtered with a nominal 10 kV focused $^{133}Cs^+$ ion beam in conjunction with normal incidence electron flooding; secondary ions were electrostatically accelerated into a mass spectrometer using a 7.5 kV extraction potential.

SIMS analyses were conducted in two different modes: as depth profiles on ion implanted materials and as spot analyses for intercomparison between materials. SIMS depth profiles were measured using a 10 µm diameter, 2 nA $^{133}Cs^+$ primary beam rastered over a 60

x 60 µm area. A 400 µm diameter field aperture was inserted into the mass spectrometer, equivalent to a 30 µm diameter field-of-view at the sample's surface. A mass resolving power of $m/\Delta m = 4400$ was used, which is sufficient to resolve ^{31}P from the nearby SiH interferences. A single depth profile typically involved 20 to 25 min of data collection. Phosphorous concentrations intrinsic to each of the samples were determined from the ratio of the stochastically modelled peak concentration within the implant profile to the background ion intensity observed at the "tail" of the profile.

For the SIMS intercomparison measurements within the NIST SRM sample series we used an unrastered 10 µm diameter, 5 nA $^{133}Cs^{+}$ beam. All other conditions were similar to those used during the depth profile analyses. A single spot analysis consisted of 8 minutes of unrastered preburn followed by 50 cycles of the peak stepping sequence of a blank mass at 29.8 Daltons (0.1 s integration), ^{30}Si (2 s) and ^{31}P (4 s), summing to a total of 7 min of data collection. The detection limit for this approach could not be directly defined due to the lack of a demonstrably 'blank' quartz sample: however, based on our low dynamic background of <2 counts per minute and the 'clean' nature of the quartz spectrum, our detection limits can be safely assumed to be well bellow the $\mu g g^{-1}$ range (see also Zinner and Crozaz 1986 for discussion of SIMS detection limits).

Concerning the accuracy of our SIMS quantitative data, we were severely hampered by the lack of a well-characterized, demonstrably homogeneous reference sample. Hence, it was first necessary for us to determine the absolute P concentration in NIST SRM 614 using an implanted sample, resulting in what may be considered a definitive concentration value. It should be noted, however, that the use of the peak height method could introduce a systematic error in the value calculated for NIST SRM 614 in that the maximum peak density was provided from a stochastic model based on SiO_2. We believe any such systematic error which might be present is small. Having thus determined an absolute P concentration in NIST SRM 614 it was possible, via the intercomparison analyses, to determine indirectly the concentrations for this element in NIST SRM 612 and 610.

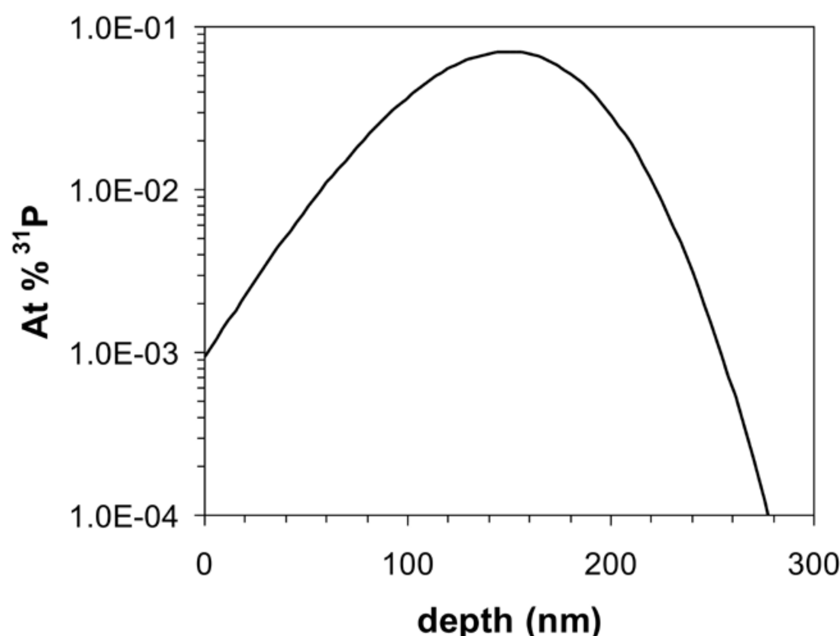

Figure 1. *Depth vs. concentration distribution of implanted 31P in crystalline SiO2 applying 100 keV and 5x1014 31P ions/cm2 based on ion-atom simulation calculation (www.srim.org). Logarithmic graph.*

2.3 Solution ICP-MS

2.3.1 HF-$HClO_4$ decomposition procedure

0.2 g of milled NIST SRM 614, 612, and 610 were weighed into Teflon vessels and moistened with 4 ml suprapure® hydrofluoric acid 40 %, and 2 ml suprapure® perchloric acid 70 %, both from Merck, before being sealed with a Teflon lid. Sample digestion was carried out with the MLS-1200 Mega microwave digestion system from Milestone. A five step microwave program was used, increasing the power from zero to 250 W, to 400 W, then to a maximum of 650 W, before decreasing the power to 250 W and finally to zero again. Each step takes five minutes. The Teflon lid was not removed before the vessel and content had been cooled down room to temperature. The content of the vessel was then transferred quantitatively to a 50 ml volumetric polymethylpentene flask.

2.3.2 Method of standard addition

Standard addition analysis is the addition of a known amount of analyte to the sample in order to determine the relative response of the detector to an analyte within the sample matrix. The difference in analytical response between the spiked and unspiked samples is due to the amount of analyte in the spike. This provides a calibration point to determine the analyte concentration in the original sample. Three solutions spiked with appropriate concentrations of P were made for each of the three NIST SRM glasses. A certified, single element standard solution of P from Spectrascan®, Teknolab A/S, Norway, was used to spike the original digested samples. A blank, digested and treated in the same way as the samples, was also prepared. The same ICP-MS as used for the LA-ICP-MS analysis was used for analysis of P in the digested NIST-glasses. Although the standard addition approach will account for matrix effects (i.e. changes in sensitivity due to the presence of matrix elements) it does not overcome “interference” issues and can therefore lead to an over-estimation of concentrations if interferences are present. However, ^{31}P at a mass resolution of 3500 m/Δm has no interference. Key instrumental parameters are given in Table 3.

***Table 3**. ICP-MS instrumental key parameters.*

ICP-MS parameters	
plasma power	965
auxiliary gas flow	1.25 l/min
sample gas flow	1.19 l/min
cone	platinum tipped
CD-2 guard electrode	Yes
injector tube	Sapphire
spray chamber	Teflon PFA
nebulizer	Teflon PFA MicroFlow
data collection	
scan type	E-scan
no. of scans	50

2.4 WDS analysis of NIST SRM 610

The P concentration in NIST SRM 610 was also determined with a LEO 1450VP scanning electron microscope equipped with an EDS-detector (Energy 400 system) and WDS-detector (Wave 500 system) from Oxford Instruments. A 10 nA beam and 15 kV acceleration voltage was employed. P concentrations were measured against an apatite mineral reference sample

from SPI Supplies which was also analyzed by wavelength dispersive spectrometry (WDS). With a peak counting time of 200 seconds and a count time of 100 seconds on both high and low background positions, the quantification limit for P is estimated to be no higher than 100 μgg^{-1}.

3. Re-evaluation of phosphorus values of RMs

3.1 Published phosphorus values of RM

Figure 2 shows two possible calibration curves for the determination of P concentration in natural quartz by LA-ICP-MS. The dashed line represents the linear weighted regression line calculated by [(cps ^{31}P/cps ^{30}Si) • conc. Si] of the RMs NIST SRM 610, 612, 614, 1830, and BAM No.1 and applying the reference P values of Pearce et al. (1997), Gao et al. (2002), and Flem and Bédard (2002; Table 1). For BAM No.1 a value of 1 μgg^{-1} P was applied, thereby covering the need for a RM with very low P. The ordinate of the calibration diagram [cps ^{31}P/cps ^{30}Si) • conc. Si] corresponds to the ^{30}Si-normalized ^{31}P signal intensity. The solid line represents the weighted regression forced through the zero intercept and using only the data from NIST SRM 610 and 612. In the past at the NGU, this procedure has been applied for calculation of P concentrations in natural quartz (e.g., Ihlen et al. 2001, 2002, 2003, 2005, Wanvik 2003, 2004, Larsen et al. 2004). The accuracy in unknown samples is poor for P concentrations <50 µgg-1 because the regression line does not pass through the origin of the calibration diagram if all 5 RMs are considered. In the case of Figure 2, the calibration curve intercepts the ordinate at 134 arbitrary units [(cps ^{31}P/cps ^{30}Si) • conc. Si]. Therefore, P concentrations in unknown samples calculated from the forced regression line are ca. 10 µgg-1 too high when <50 μgg^{-1} P is present in the sample. Based on empirical data, the P concentration of natural quartz seem frequently to be in the range of 1 to 20 μgg^{-1}, which approaches the limit of quantification for P and which makes an accurate determination challenging. The intercept of the regression line with the ordinate [(cps ^{31}P/cps ^{30}S) • conc. Si] suggests that a signal still remains after subtraction of the Ar-He background. The source of this background, which is created either during ICP plasma formation or in the vacuum interface, remains unidentified.

Equally problematical, the P values assigned to the 5 RMs form only a poorly defined a regression line, suggesting that at least two of the recommended P concentrations are significantly inaccurate. Compared to many other elements, the P concentrations of the NIST SRMs are not well defined (Hollocher and Ruiz 1995, Pearce et al. 1997, Horn et al. 1997, Rocholl et al. 1997, Sylvester 2001, Gao et al. 2002, Spandler et al. 2003, Yuan et al. 2004, Jochum et al. 2005; Table 1).

Hollocher and Ruiz (1995) determined 524±87 μgg^{-1} P in NIST SRM 611 calculated from 10 electron probe micro-analysis (EPMA). The NIST SRM 610 is chemically identical to NIST SRM 611, differing only in the thickness of the sample wafers. This concentration is exceptional high compared to the later published P values for NIST SRM 610. The recommended mean P concentration by Pearce et al. (1997) for NIST SRM 610 is based on two values which diverge greatly (Table 1). The values are 304.9±54 μgg^{-1} determined by ICP-MS and 380±9 μgg^{-1} by ICP-AES. The ICP-AES value is 25% higher than the ICP-MS value and is outside its analytical uncertainty. The NIST SRM 610 value 343±13 μgg^{-1} by Gao et al. (2002) basing on 134 LA-ICP-MS analyses is similar to the mean P concentration of Pearce et al. (1997). This is no surprise because the calibration was performed using NIST SRM 610 as an external standard with the mean P value by Pearce et al. (1997). Rocholl et al. (1997) determined 417±29 μgg^{-1} P in NIST SRM 610 by laser plasma ionization mass spectrometry (LIMS), which is 22 % higher than the mean value by Pearce et al. (1997). The mean P concentration by Pearce et al. (1997) for NIST SRM 612 is based on two values, 71.21±21.7 μgg^{-1} determined by ICP-MS and 39.1±0.6 μgg^{-1} by ICP-AES. The ICP-AES

value is 55% lower than the ICP-MS value and is well outside its analytical uncertainty. Sylvester (2001) applied 45 μgg^{-1} P for NIST SRM 612 in order to calculate P concentration in fused whole rock glasses. However, he gives no information on the source of the 45 µgg-1 P value. Spandler et al. (2003) applied 55 μgg^{-1} P for NIST SRM 612, but again no information is given how this value was established. The NIST SRM 612 value 56±7 μgg^{-1} by Gao et al. (2002) based on 15 LA-ICP-MS analyses is consistent with the mean P concentration of Pearce et al. (1997). The concentration was calibrated against NIST SRM 610 using the mean P value by Pearce et al. (1997). The P value 46±3 μgg^{-1} for NIST SRM 612 by Yuan et al. (2004) is based on the average of 4 LA-ICP-MS analyses using the Pearce et al. (1997) compiled P concentration of NIST SRM 610 for calibration. Jochum et al. (2005) recommended the value 51±6 μgg^{-1} P for NIST SRM 612 which is a compilation of the values by Pearce et al. (1997), Sylvester (2001), Gao et al. (2002), Spandler et al. (2003), and Yuan et al. (2004).

Horn et al. (1997) determined 11.8±0.1 μgg^{-1} in NIST SRM 614 by SIMS using the mean P value of Pearce et al. (1997) for NIST SRM 612 for calibration. Gao et al. (2002) published 9.3±0.1 μgg^{-1} P for NIST SRM 614. This value is based only on a single LA-ICP-MS analysis calibrated against the P concentration of NIST SRM 610 by Pearce et al. (1997). The P value, 18±2 μgg^{-1}, for NIST SRM 614 by Yuan et al. (2004) is based on the average of 4 LA-ICP-MS analyses calibrated against Pearce’s et al. (1997) mean P concentration of NIST SRM 610. Jochum et al. (2005) recommended the value 13±5 μgg^{-1} P for NIST SRM 614 which is based on a compilation of the values by Horn et al. (1997), Gao et al. (2002), and Yuan et al. (2004).

The only published P value for NIST SRM 1830 is by Flem and Bédard (2002) and is based on 8 LA-ICP-MS analyses. The mean P values of Pearce et al. (1997) for NIST SRM 610 and 612 were used for multi-RM calibration. The Federal Institute for Material Research and Testing, Germany certificate a P concentration of <1 μgg^{-1} for the RM BAM No.1 amorphous SiO_2 glass. The P concentration in the synthetic monocrystal Qz-Tu is <1 μgg^{-1} based on ~100 LA-ICP-MS analysis. The mean P values by Pearce et al. (1997; NIST SRM 610 and 612), Gao et al. (2002; NIST SRM 614), and Flem and Bédard (2002; NIST SRM 1830) were used for multi-RM calibration. The synthetic KORTH quartz crystal contains 0.13±0.02 μgg^{-1} P (Wiedenbeck unpubl.). The analysis was performed with SIMS and calibrated against the mean P value of NIST SRM 610 by Pearce et al. (1997).

A detailed assessment of the P data within the metrologic literature gives good cause for concern. Horn et al. (1997), Gao et al. (2002), Flem and Bédrad (2002) and Yuan et al. (2004) all used the reference values of NIST SRM 610 and 612 by Pearce et al. (1997) for the calibration of the P values in NIST SRM 612, 614, and 1830, respectively. The use of such poorly constrained P values would inevitably be propagated into systematic errors in the P values of NIST SRM 612, 614, and 1830. Clearly, further determination of P in the applied RM’s would be of value. For these reasons, concentrations of P in the NIST SRM glasses 610, 612, and 614 have been determined by solution ICP-MS, WDS, and SIMS. For this study it was considered crucial not to use the NIST SRM glasses themselves for calibration purposes. Therefore, standard addition was applied for solution ICP-MS, apatite for WDS, and P-implanted NIST SRM 614 and 1830 glasses and synthetic quartz for SIMS analyses

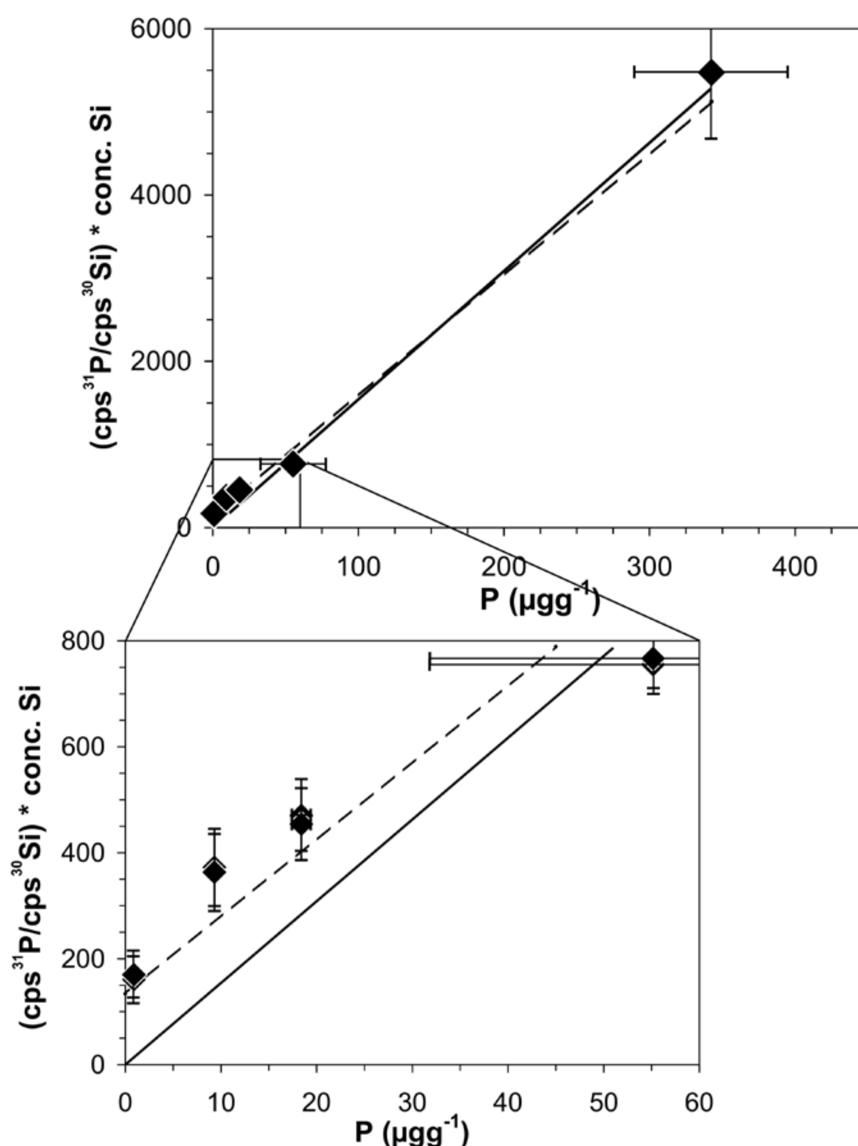

Figure 2. *Example of multi-RM calibration curve (weighted linear regression). The dashed line is the regression line calculated from [(cps ^{31}P/cps ^{30}Si) • conc. Si] values and recommended P values of the RMs NIST SRM 610, 612, 614, 1830, and BAM No.1 ("*"-values in Table 1). The P value for the BAM No.1 is set to 1 µgg^{-1} (Table 1) to have a RM with very low P. Each RM was analyzed two times. The solid line represents the regression forced through the zero intercept of the diagram by ignoring the intensities of NIST SRM 614, 1830, and BAM No.1. This procedure has been applied at the NGU for calculation of P concentrations in quartz in past years. Uncertainty bars are the standard deviations of the compiled RM P concentrations and calculated from the uncertainties of the ^{30}Si and ^{31}P signal intensities.*

3.2 Phosphorus analyses of NIST SRM glasses by solution ICP-MS and WDS

The analysis of NIST SRM 610 by standard addition solution ICP-MS and WDS gave similar values for P. Concentrations determined by standard addition solution ICP-MS are 8±2 µgg^{-1} for NIST SRM 614, 53±5 and 47±6 µgg^{-1} for NIST SRM 612, and 421±43 µgg^{-1} for NIST SRM 610. By the use of standard addition during the solution ICP-MS analyses any matrix effects are eliminated and the use of external calibration RM is not required. However,

uncertainties are introduced by the sample preparation, especially due to the need for a complete sample digestion.

Three electron probe micro-analyses gave values of 450±50, 380±40 and 450±40 $\mu g g^{-1}$ elemental P (1s uncertainties) in NIST SRM 610. The quantification was performed using an SPI Supplies apatite reference containing 18 wt.% P_2O_5. We suspect that the high P concentration in the apatite compared to the comparatively low content in NIST SRM 610 might represent a significant source of bias in our determinations, though we have been unable to quantify the likely size of any such effect.

3.3 Phosphorus analyses of NIST SRM glasses by SIMS

As mentioned above SIMS cannot directly determine elemental concentrations, rather it is only able to compare the secondary ion signals of a RM and an unknown (sample). Determining absolute concentrations employs the so-called fundamental SIMS equation which is as follows for P determination in a silicate phase:

$$\left[\frac{\dfrac{^{31}P^-}{^{28}Si^-}}{\dfrac{(P)_{atom\ ppm}}{(Si)_{atom\ \%}}}\right]_{RM} = \left[\frac{\dfrac{^{31}P^-}{^{28}Si^-}}{\dfrac{(P)_{atom\ ppm}}{(Si)_{atom\ \%}}}\right]_{unknown} \quad (1)$$

The basic assumption of this equation is that the Relative Sensitivity Factor (RSF) is constant for a given combination of two elements for a given matrix under constant analytical conditions. The RSF is dependent not only on the element and the analytical conditions, but is also dependent on the chemistry of the domain being sputtered, because the ionization efficiency varies for each element and depends on the mineral phase. SIMS analysis records the ion intensity (counts per second) as a function of the sputter time (seconds).

Figure 3 illustrates how an RSF is calculated from a depth profile using the so-called "peak high method". Briefly, the maximum count rate for $^{31}P_{max}$ from the implanted profile is determined, from which the background rate intrinsic to the sample $^{31}P_{int}$ is subtracted. This corrected count rate, the observed $^{30}Si^-$ count rate, the maximum P concentration in at% obtained from the ion simulation and the known atomic concentration of Si in quartz (33.3 %) are used to calculate the RSF needed by eqn. 1.

Relative sensitivity factors derived from the ^{31}P-implanted samples are compared in Table 4. The concentrations of the P intrinsic to each of the three ^{31}P-implanted RMs were then calculated by applying formula (1) to the $^{31}P^-/^{28}Si^-$ observed at the "tail" of the analysis. The calculated P concentrations of NIST SRM 1830 and 614 are in good agreement with the published preferred values (compare with Table 1). Absolute concentrations of P in the NIST SRM 612 and 610 were subsequently determined by using the newly derived P content of NIST SRM 614 and comparing the $^{31}P^-/^{28}Si^-$ signal intensities between non-implanted NIST SRM 614 and those obtained on SIST SRM 612 and 610. The results are listed on Table 5. The obtained SIMS data for the NIST SRM 614 are in good agreement whereas the concentrations for NIST SRM 612 and 610 are respectively significantly lower and higher than preferred values of Pearce et al. (1997). It is noted, though, that the new SIMS concentrations values fall in the range of the mean values given by Pearce et al. (1997)

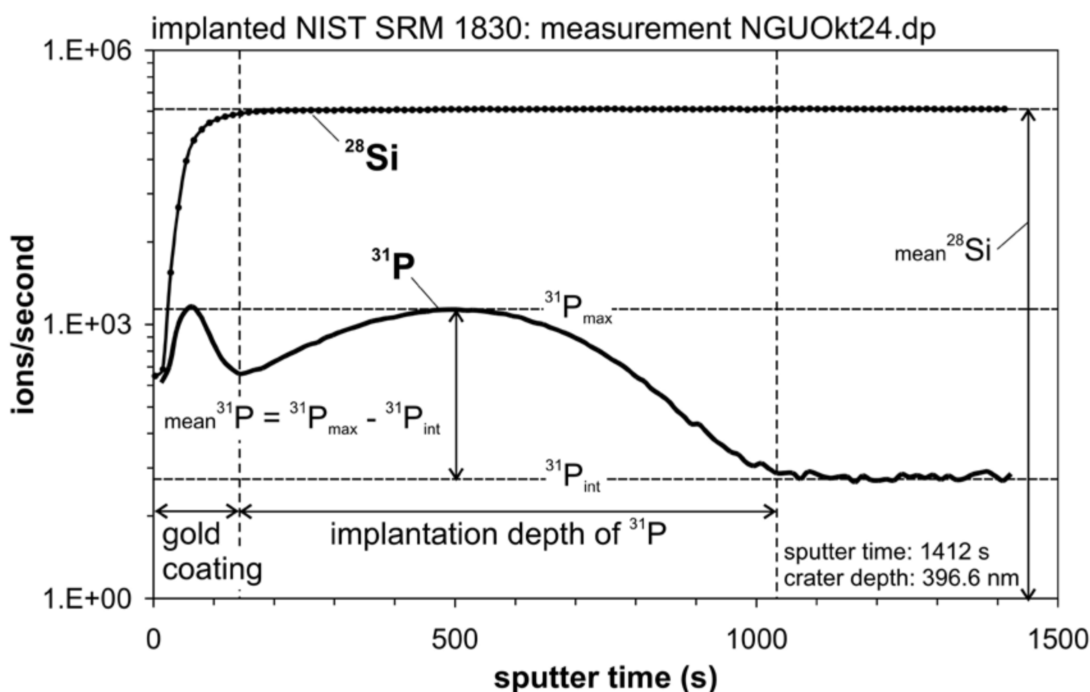

Figure 3. *An example of a profile analysis for the ^{31}P-implanted NIST SRM 1830. By assuming a constant sputtering rate and knowing the total duration and final depth of the analysis, the peak implant depth can be estimated at ~140 nm.*

Table 4*. Relative sensitivity factors (RSF) of 31P-implanted reference materials and the calculated P content (Pcalc) of these samples. SD – standard deviation of the P concentration.*

sample	**analysis date**	**nr. of analyses**	**RSF**	**SD**	**Si (atom %)**	**P_{calc} (µgg^{-1})**	**SD**
NIST SRM 1830	23.10.2006	10	2.137	0.130	25.1	16.7	1.5
NIST SRM 614	23.10.2006	10	2.015	0.045	25.0	8.5	0.8
synthetic quartz KORTH	06.10.2005	2	1.372	0.085	33.3	0.4	0.1

Table 5. *Ratios and absolute concentrations of P in NIST SRM 610, 612, and 614 determined by SIMS and compared with recommended concentration values by Pearce et al. (1997) and Gao et al. (2002).*

material	**SIMS analyses October 2006**				**published reference values**		
	^{31}P/^{28}Si	P ratio	P (µgg^{-1})	SD	P ratio	P (µgg^{-1})	SD
NIST SRM 614	4.63E-05	1	8.5	0.8	1	9.3*	0.1
NIST SRM 612	2.08E-4	4.49	38.3	1.8	5.92	55.2**	22.7
NIST SRM 610	2.16E-3	46.6	398	35	36.79	342**	53

* - Gao *et al.* (2002); ** - Pearce *et al.* (1997)

3.4 Proposed new phosphorus values for NIST SRM 610, 612, 614, and 1830

The P concentrations determined for NIST SRM 610, 612, 614, and 1830 in this study are generally within the uncertainty range of previously published P values. However, the use of P-implanted samples has allowed us to determine the P concentrations independently of the published values, thus eliminating concerns about the accuracy of previously published data. The newly compiled P values for the RM glasses are shown in Table 1 in orange. Some of the published P values are excluded from the compilation because of poorly documented analytical procedures, outstanding concentrations compared to majority of published values (e.g., Hollocher and Ruiz 1995) or because they represent values based exclusively on already published concentrations (e.g., Jochum et al. 2005; Table 1). Our recommended P concentrations are 409 μgg^{-1} for NIST SRM 610, 45.9 μgg^{-1} for NIST SRM 612, 11.1 μgg^{-1} for NIST SRM 614, and 16.6 μgg^{-1} for NIST SRM 1830 (see Table 1 for uncertainty values). Compared to our earlier efforts, the four compiled standard values give a much improved linear regression if plotted against (cps ^{31}P/cps ^{30}Si) • conc. Si (Figure 4).

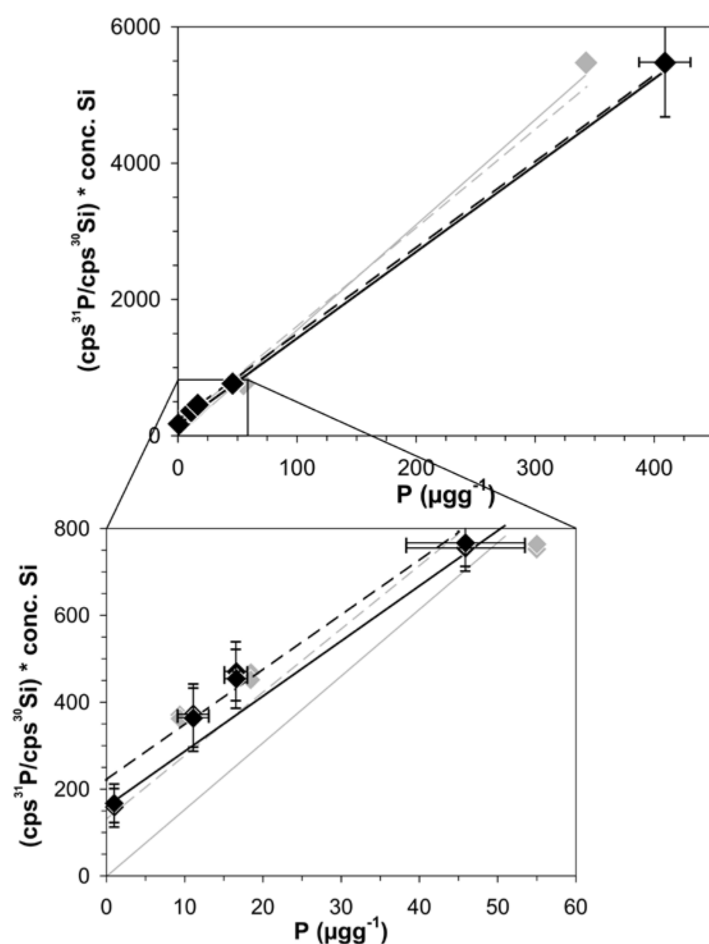

Figure 4. Multi-standard calibration curve (black dashed line) applying the newly compiled P values of the RMs NIST SRM 610, 612, 614, and 1830. The dataset is the same as in Figure 2 shown as gray diamonds and lines in the background. The black solid line represents the weighted linear regression with corrected intercept b.

4. Discussion of the ICP-MS related background at mass ^{31}P

4.1 Spectroscopic interference of ^{31}P with silicon hybrids and other compounds created during ionization

At a mass of 30.9738 Daltons ^{31}P can be severely affected by the polyatomic interferences $^{15}N^{16}O^{+}$, $^{1}H^{14}N^{16}O^{+}$, and silicon hybrids. Mass resolutions of $m/\Delta m = 1458$ and 967 are necessary to resolve interferences with $^{15}N^{16}O^{+}$ and $^{1}H^{14}N^{16}O^{+}$, respectively. Thus, the applied mass resolution of ca. 3500 $m/\Delta m$ was sufficient to resolve these interferences. Trace amounts of several Si-H species are created from silicate minerals and glasses during ionization (e.g., Koshi et al. 1991), which can cause interferences with ^{31}P. The Si-H species $^{30}Si^{1}H$ with the mass 30.9816 Daltons is very close to the mass of ^{31}P requiring a mass resolution of $m/\Delta m = 3951$ for complete separation. The applied mass resolution of ca. 3500 $m/\Delta m$ results in only a small mass peak overlap with $^{30}Si^{1}H$. However, only the central part of the 31P mass peak has been used for data reduction, excluding the area of overlap. Figure 5 shows the mass peaks around 31P during the ablation of NIST SRM 610. The mass peak of $^{30}Si^{1}H$ is hardly developed in reality and no mass interferences were detected.

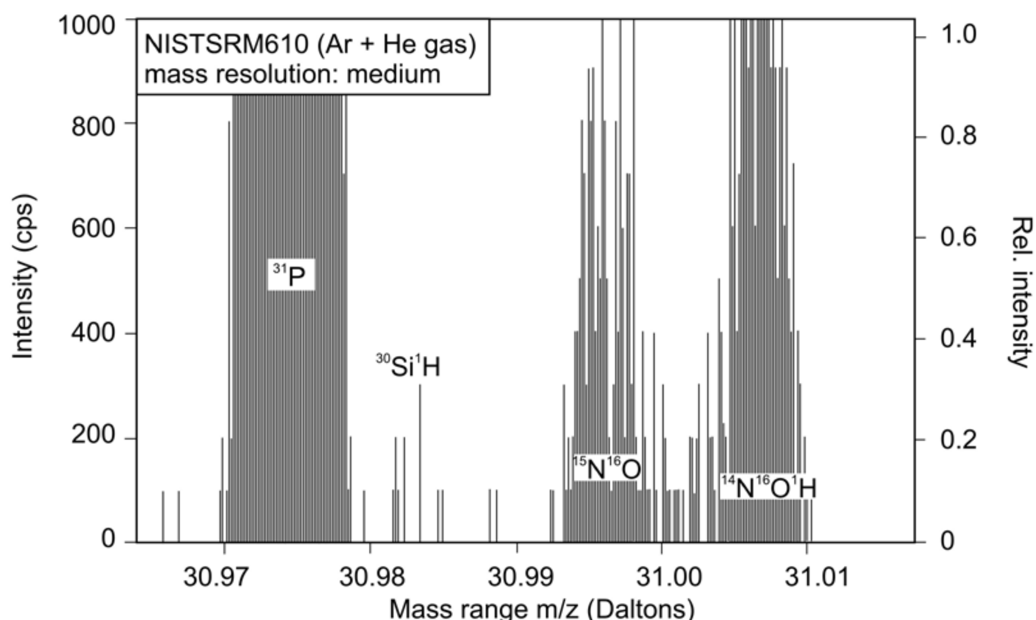

***Figure 5**. Resolution of mass peaks around ^{31}P during ablation of NIST SRM 610 at medium mass resolution ($m/\Delta m = 3500$).*

4.2 Spectroscopic interference of the internal standard ^{30}Si

^{30}Si was used as an internal standard at medium mass resolution. At $m/\Delta m$ all significant isobaric interferences are eliminated from the ^{30}Si mass station, meaning that this species is highly suitable as an internal standard.

4.3 Phosphorus fractionation during ablation, transport and ionization

Some elements (e.g., Cd, Zn) show an increase in signal intensity relative to a less volatile element (e.g., Ca) as a function of time during prolonged laser ablation (Gray 1985, Fryer et

al. 1995). Fryer et al. (1995) and Guillong and Günther (2003) observed ^{31}P elemental fractionation relative to Ca as the ablation progresses deeper into the samples. The underlying phenomenon causing elemental fraction effects can originate during ablation, during aerosol transport or during vaporization, atomization and ionization within the ICP torch. Mank and Mason (1999) demonstrated that a critical crater depth : diameter ratio of >6 leads to an enhanced mobilization of volatile elements and therefore to pronounced elemental fractionation. The application of the raster technique at the NGU results in a crater depth to diameter ratio between 1 and 3. The raster mode has been demonstrated to reduce substantially time-dependent variation of signal intensities (Fryer et al. 1995). It therefore seems likely that laser-induced fraction of P due to an excessive crater aspect ratio is not significant. However, during rastering the laser beam is not only hitting pristine sample surfaces but also ablates sample ejecta from the preceding ablation. Such ejecta might be already fractionated compared to the composition of the sample (Košler et al. 2005).

Kuhn and Günther (2004), Kuhn et al. (2004) and Aeschliman et al. (2003) showed that the size of the ablated particles has a significant influence on the vaporization, atomization and ionization within the ICP. Therefore, size-dependent composition and incomplete vaporization of particles larger than 150 nm (glass particles) within the ICP leads to elemental fractionation effects. Broad particle size distribution occurs mainly at the beginning of the ablation (Kroslakova 2006). An incomplete vaporization of such large particles within the torch seems to be the dominating effect during the first 10 to 20 seconds of ablation and overprints the ICP-induced matrix effects. The measurements we performed at NGU are started only after 30 seconds of ablation to minimize the particle size effect. However, the applied raster scan is continually hitting pristine sample surface which may result in fluctuating particle sizes.

An additional issue which needs consideration is the fact that the optical coupling of the NIST SRMs and crystalline quartz are different, recognizable by differences in the depth of the ablation craters. The most absorbing glass, NIST SRM 610, has the lowest depth of photon penetration and therefore the lowest ablation rate. In contrast, NIST SRM 614, a more transparent material, ablates twice as fast (Guillong and Günther 2003), leading to differences in both the mass load of the plasma and particle size distribution: so-called matrix effects. Such matrix effects can occur during the laser sampling, during the aerosol transport into the ion source or inside the plasma (Longerich et al. 1996, Chen 1999, Russo et al. 2000, Koch et al. 2002, Guillong and Günther 2003). Matrix effects result not only from the size of the particles but also from the amount of sample introduced into the plasma, since this has an effect on plasma temperature and therefore on ionization efficiency. Guillong and Günther (2003) proved that variations in the ionization efficiency of different sized particles generated during the ablation of silicates do occur. Mass load induced matrix effects have been described for elements with low melting points (Kroslakova and Günther 2006). Thus, P would be expected to be sensitive to this effect. Internal standardization is not suitable for correcting mass load dependent matrix effects and element dependent sampling efficiency into the mass spectrometer, especially when ions are generated within different zones of the plasma (e.g., Kroslakova and Günther 2007). Therefore, quantitative analyses should only be carried out using the same input parameters for crater diameter, ablation rate and ablation time for both the RM and the sample. This is standard procedure for LA-ICP-MS analyses conducted at the NGU. As discussed before, RM and samples have different ablation rates depending on their laser absorptivity. To obtain similar ablation rates the laser energy must be adjusted to each material. However, the ablation rate varies from sample to sample and it is therefore not exactly adjustable.

Summarizing, minor laser- and plasma-induced matrix effects and particle size effects might impair the accuracy of determined P concentrations. These effects are possibly reflected in the

poorly defined linear regression of the multi-RM calibration curves (Figure 2) but do not explain why the calibration curve does not pass the origin of the normalized intensity vs. concentration diagram. The unsatisfying regression line may also be caused, at least in part, by the inaccurate published P concentrations of the reference materials as discussed below.

4.4 Other possible causes of the ICP-MS related background

Table 6 lists the Ar-He background, the 31P intensity with subtracted Ar-He background, and (cps ^{31}P/cps ^{30}Si) • conc. Si of NIST SRM glasses, the synthetic Qz-Tu quartz and BAM No.1, and one natural quartz (sample) for 15 analysis sequences carried out during the last three years at the NGU.

The Ar-He background intensities are similar for glasses, synthetic and natural quartz. Minor memory effects are observed for the Ar-He background of the NIST SRM 1830 because the P-rich NIST SRM 610 is measured immediately prior to NIST SRM 1830 during the analysis sequence developed by the NGU.

A comparison of the data reveals that the [(cps ^{31}P/cps ^{30}Si) • conc. Si] values of the Qz-Tu quartz and BAM No.1 with <1 µgg^{-1} P are too high. The high values of the P-poor RMs cause the best-fit calibration curve to transect the ordinate between 100 and 500 arbitrary units [(cps ^{31}P/cps ^{30}Si) • conc. Si] (Figure 2). Ideally, the calibration curve should transect the ordinate at zero. The [(cps ^{31}P/cps ^{30}Si) • conc. Si] values of RMs with low P indicate that a ^{31}P-background is created during plasma formation and/or during ablation and aerosol transport. The ICP-MS related background might be introduced through hardware of the mass spectrometer such as the cone or extraction lens, which may contain some trace amounts of P. However, the gas blank is uniform for each analysis sequence and significant lower than the signal intensities for the low P (<1 µgg^{-1}) RMs Qz-Tu, SiO_2 blank and BAM No. 1 (Table 6), which might indicate that the instrument hardware is not the source of the P background. This is supported by the solution ICP-MS measurements for which no anomalously high background values were observed. The measurements were carried out on the same mass spectrometer.

Because the background is independent of the type of RMs and samples, it may be induced during sample preparation. However, samples measured at NGU are routinely prepared in four different laboratories using different mounting and polishing procedures. Sample surfaces are carefully cleaned with pure ethanol before measurement. Thus, contamination of P analyses by foreign substances on the sample surface seems highly unlikely. In conclusion, the origin of the observed ^{31}P background remains unclear.

Table 6. *Ar-He background, ^{31}P intensity with subtracted Ar-He background, the [(cps ^{31}P/cps ^{30}Si) • conc. Si] value (^{30}Si-normalized ^{31}P signal intensity) of RMs, and parameters of the calibration curve (weighted regression: slope a, intercept b, correlation coefficient R2) obtained during the last three years at NGU b corr – corrected intercept by adapting to the P concentration of the Qz-Tu quartz and BAM No. 1 to 1 µgg^{-1}, LOD – limit of detection (3 sigma), LOD sample – reference sample used for LOD determination, SiO_2 bl. – SiO_2 blank sample, sequ. – analysis sequence, n – number of scans, * - SiO_2 blank with <1 µgg^{-1} P were analyzed in place of Qz-Tu.*

		P conc.	sequ.	2007 0147C	2007 0147B	2007 0147A	2006 0498A	2006 0478B	2006 0478A	2006 0065C	2006 0065B	2006 0065A	2005 0144D	2005 0144C	2005 0144B	2005 0102C	2005 0102B	2005 0102A
		µgg^{-1}	date	21.06. 2007	31.05. 2007	29.05. 2007	13.12. 2006	06.12. 2006	22.11. 2006	09.03. 2006	21.02. 2006	16.02. 2006	09.06. 2005	08.06. 2005	02.06. 2005	20.04. 2005	30.03 2005	17.03. 2005
Ar-He background of ^{31}P (cps)	**Qz-Tu**	**1**	n=40	447*	381*	377	784	780	847	761	465	306	n.d.	511	693	282	271	447
	BAM No.1	**1**	n=40	410	387	387	928	851	869	942	630	336	633	525	869	313	345	523
	NIST 614	**11.1**	n=40	454	391	374	848	708	876	804	539	261	568	346	690	261	289	401
	NIST 612	**45.9**	n=40	445	412	396	940	812	855	795	536	264	555	377	629	315	284	454
	NIST 610	**409**	n=40	419	401	382	862	835	836	794	520	273	557	363	636	294	295	430
	NIST 1830	**16.6**	n=40	494	478	431	936	826	905	874	548	281	568	350	733	307	297	407
	sample		n=20	444	503	404	935	848	930	923	551	292	753	336	695	298	282	460
^{31}P intensity with subtracted Ar-He background (cps)	**Qz-Tu**	**1**	n=40	990*	951*	1010	1594	1000	1220	2414	2471	970	n.d.	1029	1592	608	883	1137
	BAM No.1	**1**	n=40	1037	883	1097	1583	1223	1393	3929	3297	1446	2025	2335	2518	1119	1106	1358
	NIST 614	**11.1**	n=40	3011	2756	2742	2987	2089	2723	5043	4264	2100	2639	2030	2894	1162	1384	2114
	NIST 612	**45.9**	n=40	6692	5806	5432	4932	3946	5237	7800	7535	5326	5389	4467	5659	3459	3343	4502
	NIST 610	**409**	n=40	60267	53317	47391	36562	30645	34047	51132	62546	53350	51551	46359	47790	35845	34448	48784
	NIST 1830	**16.6**	n=40	3135	3084	2605	2392	2387	2689	4703	4436	2941	2608	2389	3349	1669	1671	2072
(cps ^{31}P/cps ^{30}Si) • conc. Si	**Qz-Tu**	**1**	n=40	97*	101*	155	285	166	154	503	258	124	n.d.	177	180	125	95	149
	BAM No.1	**1**	n=40	106	91	152	247	165	171	704	331	154	195	269	240	214	143	153
	NIST 614	**11.1**	n=40	293	303	360	475	368	379	743	436	244	292	238	299	219	201	261
	NIST 612	**45.9**	n=40	622	599	639	829	767	735	1129	769	600	660	563	558	550	471	540
	NIST 610	**409**	n=40	4743	4374	4516	5420	5469	5327	5519	4830	4677	4232	4275	4300	4576	3652	4372
	NIST 1830	**16.6**	n=40	320	308	332	430	462	417	714	493	342	302	315	396	293	258	256
parameters of the calibration curve (weighted regression)	***a***			11.24	10.26	10.53	12.55	12.7	12.39	12.14	11.05	11.08	9.99	10.11	9.94	10.94	8.66	10.39
	b			138	156	199	274	221	217	555	302	134	164	130	183	89	103	108
	b_{corr}			108	94	155	246	160	160	528	287	112	172	160	200	122	103	120
	R^2			0.9996	0.9986	0.9979	0.9977	0.9981	0.9984	0.9987	0.9997	0.9991	0.9985	0.9995	0.9944	0.9995	0.9996	0.9984
LOD			µgg^{-1}	2	1	3.4	6.5	3.5	2.6	7.2	9.4	2	6.6	3.1	2	3.3	3.6	2.7
LOD sample				SiO_2 bl.	SiO_2 bl.	Qz-Tu	Qz-Tu	Qz-Tu	Qz-Tu	Qz-Tu	Qz-Tu	Qz-Tu	Qz-Tu	Qz-Tu	Qz-Tu	Qz-Tu	Qz-Tu	Qz-Tu

5. Conclusions and outlook

The newly compiled P values for NIST SRM 610, 612, 614, and 1830 (Table 1) define a better calibration curve compared to the recommended P values by Pearce et al. (1997), Gao et al. (2002), and Flem and Bédard (2002). The compiled values exclude previously published P concentrations for which the analytical procedure were not adequately documented, concentrations which are clearly divergent for the majority of published values, and compilations which are based only on already published concentrations.

Ideally, the calibration curve should go through the zero point of the calibration diagram (intercept $b = 0$). However, the calibration curve transects the [(cps ^{31}P/cps ^{30}Si) • conc. Si] ordinate between 89 and 555 arbitrary units (Table 6). Thus, the newly compiled P values of the reference materials do not solve the problem of the ICP-MS related background.
From the data represented in Table 6 it is clear that the background, represented by the intercept b, is added to the signal during plasma formation. The intercept b, which corresponds to the ICP-MS related background, should be slightly lower than the [(cps ^{31}P/cps ^{30}Si) • conc. Si] value of the Qz-Tu quartz and BAM No.1, which contain <1 $\mu g g^{-1}$ P (Table 1). However, the intercept b is somewhat higher for the measurement sequences 2007/2006 and somewhat lower for the measurement sequences 2005. The higher intercept b results in negative P concentrations for the Qz-Tu quartz and BAM No.1. Therefore, the intercept b is manually adapted in such a way that the calculated concentrations of the Qz-Tu quartz and BAM No.1 are ca. 1 $\mu g g^{-1}$ P. The results of the adaptation are given as intercept b corr. (Table 6).

In future the intercept b will be subtracted from the [(cps ^{31}P/cps ^{30}Si) • conc. Si] value for calibration of absolute P concentrations in crystalline quartz at NGU. The calibration curve should not be forced through the origin of the calibration diagram. In most of the cases, the intercept b has to be slightly corrected for each analysis sequence such that the calculated P concentrations for the Qz-Tu quartz and BAM No.1 are ca. 1 $\mu g g^{-1}$.

6. Acknowledgements

The authors are grateful to two anonymous reviewers for their constructive comments.

7. References

Aeschliman D.B., Bajic S.J., Baldwin D.P. and Houk R.S. (2003) High-speed digital photographic study of an ICP during laser ablation: Comparison of dried solution aerosols from a microconcentric nebulizer and solid particles from laser ablation. Journal of Analytical Atomic Spectrometry, 18, 1008-1014.

Chen Z.X. (1999) Inter-element fractionation and correction in laser ablation inductively coupled plasma mass spectrometry. Journal of Analytical Atomic Spectrometry 14, 1823-1828.

Dash K., Thangavel S., Rao S.V., Chandrasekaran K., Chaurasia S.C. and Arunachalam J. (2004) Ion chromatographic determination of trace level phosphorus in purified quartz. Journal of Chromatography A, 1036, 223-227.

Dick W.A. and Tabatabai M.A. (1977) Determination of orthophosphate in aqueous solutions containing labile organic and inorganic phosphorus compounds. Journal of Environmental Quality, 6, 82-85.

Dietl J., Helmreich D. and Sirtl E. (1981) "Solar" silicon. In: Crystals: Growth Properties and Applications. Springer (Berlin) Vol. 5, 43-107.

Feldmann I., Tittes W., Jakubowski N., Stuewer D. and Giessmann U. (1994) Performance characteristics of inductively-coupled plasma-mass spectrometry with high-mass resolution. Journal of Analytical Atomic Spectrometry, 9, 1007-1014.

Flem B. and Bédard L.P. (2002) Determination of trace elements in BCS CRM 313/1 (BAS) and NIST SRM 1830 by inductively coupled plasma-mass spectrometry and instrumental neutron activation analysis. Geostandards Newsletter, 26, 287-300.

Flem B., Larsen R.B., Grimstvedt A. and Mansfeld J. (2002) In situ analysis of trace elements in quartz by using laser ablation inductively coupled plasma mass spectrometry. Chemical Geology, 182, 237-247.

Fryer B.J., Jackson S.E. and Longerich H.P. (1995) The design, operation and role of the laser-ablation microprobe coupled with an inductively coupled plasma-mass spectrometer (LAM-ICP-MS) in the earth sciences. Canadian Mineralogist, 33, 303-312.

Gao S., Liu X., Yuan H., Hattendorf B., Günther D., Chen L. and Hu S. (2002) Determination of forty-two major and trace elements in USGS and NIST SRM glasses by laser ablation-inductively coupled plasma-mass spectrometry. Geostandards Newsletter, 26, 181-196.

Gießmann U. and Greb U. (1994) High resolution ICP-MS - a new concept for elemental mass spectrometry. Fresenius' Journal of Analytical Chemistry, 350, 186-193.

Götze J., Plötze M. and Habermann D. (2001) Origin, spectral characteristics and practical applications of the cathodoluminescence (CL) of quartz – a review. Mineralogy and Petrology, 71, 225-250.

Gray A.L. (1985) Solid sample introduction by laser ablation for inductively coupled plasma source mass spectrometry. Analyst 110, 551-556.

Guillong M. and Günther D. (2002) Effect of particle size distribution on ICP-induced elemental fractionation in laser ablation-inductively coupled plasma-mass spectrometry. Journal of Analytical Atomic Spectrometry, 17, 831-837.

Günther D. and Heinrich C.A. (1999) Enhanced sensitivity in LA-ICP-MS using helium-argon mixtures as aerosol carrier. Journal of Analytical Atomic Spectrometry, 14, 1369-1374.

Hollocher K. and Ruiz J. (1995) Major and trace element determinations on NIST glass standard reference materials 611, 612, 614 and 1834 by inductively coupled plasma-mass spectrometry. Geostandards Newsletter, 19, 27-34.

Horn I., Hinton R.W., Jackson S.E. and Longerich H.P. (1997) Ultra-trace element analysis of NIST SRM 616 and 614 using laser ablation microprobe inductively coupled plasma

mass spectrometry (LAM-ICP-MS): a comparison with secondary ion mass spectrometry (SIMS). Geostandards Newsletter, 21, 191-203.

Ihlen P.M., Lynum R., Henderson I. and Larsen R.B. (2001) Potensielle ressurser av kvarts- og feldspat- råstoffer på Sørlandet, I: Regional prøvetaking av utvalgte feltspatbrudd i Frolandsområdet. Norwegian Geological Survey Report 2001.044 (Trondheim), 46pp.

Ihlen P.M., Henderson I., Larsen R.B. and Lynum R. (2002) Potensielle ressurser av kvarts- og feldspat- råstoffer på Sørlandet, II: Resultater av undersøkelsene i Frolandsområdet i 2001. Norwegian Geological Survey Report 2002.009 (Trondheim), 28pp.

Ihlen P.M., Henderson I., Larsen R.B., Lynum R. and Furuhaug L. (2003) Potentielle ressurser av kvarts- og feldspat-råstoffer på Sørlandet, III: Sporelementsammensetningen av pegmatittisk og hydrothermal kvarts i Froland, Østre Froland of Lillesand. Status quo ved utgangen av 2002. Norwegian Geological Survey Report 2003.035 (Trondheim), 38pp.

Ihlen P.M., Furuhaug L., Lynum R., Müller A. and Larsen R.B. (2005) Gitterbundete sporelementer i kvarts fra pegmatitter, hydrotermale ganger, kvartsitter og granitter i Sør-Norge. Norwegian Geological Survey Report 2004.020 (Trondheim), 49pp.

Jochum K.P., Nohl U., Herwig K., Lammel E., Stoll B. and Hofmann W. (2005) GeoReM: A new geochemical database for reference materials and isotopic standards. Geostandards and Geoanalytical Research, 29, 333-338.

Koch J., Feldmann I., Jakubowski N. and Niemax K. (2002) Elemental composition of laser ablation aerosol particles deposited in the transport tube to an ICP. Spectrochimica Acta Part B, 57, 975-985.

Korth Kristalle GmbH (2007) Korth Kristalle GmbH. Accessed 23th January 2007. <http://korth.de/eng/index.htm>

Koshi M., Miyoshi A. and Matsui H. (1991) Kinetics of the SiH3 + O2 reaction studied by time-resolved mass spectrometry. Journal of Physical Chemistry, 95, 9869-9873.

Košler J., Wiedenbeck M., Wirth R., Hovorka J., Sylvester P. and Míková J. (2005) Chemical and phase composition of particles produced by laser ablation of silicate glass and zircon – implications for elemental fractionation during ICP-MS analysis. Journal of Analytical Atomic Spectrometry, 20, 402-409.

Kroslakova I. (2006) Plasma related matrix effects in LA-ICP-MS. PhD thesis, Eidgenössische Technische Hochschule ETH Zürich, Nr. 16751. Accessed 19th October 2007 <http://e-collection.ethbib.ethz.ch/show?type=diss&nr=16751>.

Kroslakova I. and Günther D. (2007) Elemental fractionation in laser ablation-inductively coupled plasma-mass spectrometry: evidence for mass load induced matrix effects in the ICP during ablation of a silicate glass. Journal of Analytical Atomic Spectrometry, 22, 51-62.

Kuhn H.R. and Günther D. (2004) Laser ablation-ICP-MS: particle size dependent elemental composition studies on filter-collected and online measured aerosols from glass. Journal of Analytical Atomic Spectrometry, 19, 1158-1164.

Kuhn H.R., Guillong M. and Günther D. (2004) Size-related vaporisation and ionisation of laser-induced glass particles in the inductively coupled plasma. Analytical and Bioanalytical Chemistry, 378, 1069-1074.

Larsen R.B., Henderson I., Ihlen P.M. and Jacamon F. (2004) Distribution and petrogenetic behaviour of trace elements in granitic pegmatite quartz from South Norway. Contributions to Mineralogy and Petrology, 147, 615-628.

Longerich H.P., Günther D. and Jackson S.E. (1996) Elemental fractionation in laser ablation inductively coupled plasma mass spectrometry. Fresenius' Journal of Analytical Chemistry, 355, 538-542.

Mank A.J.G. and Mason P.R.D. (1999) A critical assessment of laser ablation ICP-MS as an analytical tool for depth analysis in silica-based samples. Journal of Analytical Atomic Spectrometry 14, 1143-1153.

Müller A., Wiedenbeck M., Van den Kerkhof A.M., Kronz A. and Simon K. (2003) Trace elements in quartz – a combined electron microprobe, secondary ion mass spectrometry, laser-ablation ICP-MS, and cathodoluminescence study. European Journal of Mineralogy, 15, 747-763.

Panalytic GmbH Dresden (2007) Panalytic Material- und Strukturanalysen GmbH Niederlassung Dresden. Accessed 23th January 2007. <http://www.panalytic.com>.

Pearce N.J.G., Perkins W.T., Westgate J.W., Gorton M.P., Jackson S.E., Neal C.R. and Chenery S.P. (1997) A compilation of new and published major and trace element data for NIST SRM 610 and NIST SRM 612 glass reference materials. Geostandards Newsletter, 21, 115-144.

Potts P.J. (1997) A glossary of terms and definitions used in analytical chemistry. Geostandards Newsletter, 21, 157-161.

Rocholl A.B.E., Simon K., Jochum K.P., Bruhn F., Gehann R., Kramar U., Luecke W., Molzahn M., Pernicka E., Seufert M., Spettel B., Stummeier J. (1997) Chemical characterisation of NIST silicate glass certified reference material SRM 610 by ICP-MS, TIMS, LIMS, SSMS, INAA, AAS and PIXE. Geostandards Newsletter, 21, 101-114.

Russo R.E., Mao X.L., Borisov O.V. and Haichen L. (2000) Influence of wavelength on fractionation in laser ablation ICP-MS. Journal of Analytical Atomic Spectrometry, 15, 1115-1120.

Schroeder E., Hamester M. and Kaiser M. (1998) Properties and characteristics of a laser ablation ICP-MS system for the quantitative elemental analysis of glasses. Applied Surface Sciences, 127-129, 292-298.

Schrön W., Baumann L. and Rank K. (1982) Zur Charakterisierung von Quarzgenerationen in den postmagmatogenen Erzformationen des Erzgebirges. Zeitschrift für Geologische Wissenschaften, 10/12, 1499-1521.

Spandler C., Hermann J., Arculus R. and Mavrogenes J. (2003) Redistribution of trace elements during prograde metamorphism from lawsonite blueschist to eclogite facies; implications for deep subduction-zone processes. Contributions to Mineralogy and Petrology, 146, 205-222.

Sylvester P. (2001) Trace element analysis of fused whole rock glasses by laser ablation ICPMS. In: Sylvester P. (ed), Laser-Ablation-ICPMS in the Earth Sciences. Short-course vol. 29, Mineralogical Association of Canada, 147-162.

Wanvik J.E. (2003) Nasafjell kvartsforekomst. Norwegian Geological Survey, Report 2003.047 (Trondheim), 23pp.

Wanvik J.E. (2004) Supplerende kvartsundersøkelser på Saltfjellet. Norwegian Geological Survey, Report 2003.106 (Trondheim), 32pp.

Yuan H., Gao S., Liu X., Li H., Günther D. and Wu F. (2004) Accurate U-Pb age and trace element determinations of zircon by laser ablation-inductively coupled plasma-mass spectrometry. Geostandards and Geoanalytical Research, 28/3, 353-370.

Zinner E. and Crozaz G. (1986) A method for the quantitative measurement of rare earth elements in the ion microprobe. International Journal Mass Spectrometry and Ion Processes, 69, 17-38.